

Soap-film flow induced by electric fields in asymmetric frames

S. Mollaei, M. Nasiri,* and N. Soltanmohammadi

Department of Physics, Faculty of Science, University of Zanjan, Zanjan P.O. Box 45371-38791, Iran

R. Shirsavar

*Department of Physics, Faculty of Science, University of Zanjan, Zanjan P.O. Box 45371-38791, Iran
and Department of Physics, Sharif University of Technology, Tehran P.O. Box 11365-9161, Iran*

A. Ramos

Departamento de Electrónica y Electromagnetismo, Facultad de Física, Universidad de Sevilla, Seville 41012, Spain

A. Amjadi

Department of Physics, Sharif University of Technology, Tehran P.O. Box 11365-9161, Iran

(Received 1 July 2017; published 17 April 2018)

Net fluid flow of soap films induced by (ac or dc) electric fields in asymmetric frames is presented. Previous experiments of controllable soap film flow required the simultaneous use of an electrical current passing through the film and an external electric field or the use of nonuniform ac electric fields. Here a single voltage difference generates both the electrical current going through the film and the electric field that actuates on the charge induced on the film. The film is set into global motion due to the broken symmetry that appears by the use of asymmetric frames. If symmetric frames are used, the film flow is not steady but time dependent and irregular. Finally, we study numerically these film flows by employing the model of charge induction in ohmic liquids.

DOI: [10.1103/PhysRevE.97.043110](https://doi.org/10.1103/PhysRevE.97.043110)**I. INTRODUCTION**

The control and manipulation of small masses of liquids by using electric fields have been widely studied because of many promising applications in micro-electromechanical industry, chemical analysis, and/or biotechnology [1–3]. Lab-on-chip devices with integrated pumps, reagent dispensers, mixers, separators, and detection units could benefit greatly from the use of electric fields [4,5]. In this regard, soft nanofluidic channels of nanometric thickness that are found in soap films can substitute for solid channels in microdevices, with the advantage that in addition to the conventional solid walls, the electroosmotic flows can be generated in these soft liquid nanochannels [6]. Electrokinetic transport and detailed characteristics of soap films are discussed in a recent review article [7].

Gharib *et al.* [8], Chomaz *et al.* [9], and Rutgers *et al.* [10] have studied soap film flows as two-dimensional complex fluid flows. In these studies, the dominant forces were gravity, surface tension, and surface-air interaction. Fluid flows induced by electric fields in films made of complex structured fluids have been studied by Faetti *et al.* [11,12] and Morris *et al.* [13,14]. The flow of an electric current through nematic and smectic freely suspended liquid crystal films was shown to induce vortices on the film. Amjadi *et al.* [15] demonstrated a continuous rotating flow on suspended water films by using, simultaneously, a current passing through the liquid film and

an external electric field perpendicular to and in the plane of the electrical current. The continuous rotation of fluid films has also been reported for polar liquid [16] and MBBA [*N*-(4-methoxybenzylidene)-4-butylaniline] liquid crystal [17] films. Saghaei *et al.* [18] studied a related experiment of liquid bulk rotation with one free surface. Nasiri *et al.* have proposed an explanation of the water film rotation based on the electrical forces actuating on charges induced on the free surface of an ohmic liquid [19]. AC electric fields were also shown to generate flows in soap films by the charge induction mechanism of ohmic liquids [20,21].

This paper presents experiments on net fluid flow of soap films induced by (ac or dc) electric fields in asymmetric frames. Previous experiments of controllable soap film flow required the simultaneous use of an electrical current passing through the film and an external electric field [15] or the use of ac nonuniform electric fields at kilohertz frequencies [20]. Here the same voltage difference generates both the electrical current going through the film and the electric field that acts on the charge induced on the film. In the present experiments, we use frames with asymmetric apertures with the idea that the film will be set into global motion due to the broken symmetry, as happens in other situations [22,23]. The paper is organized as follows. First, we present the experiments using symmetric frames, which do not show controllable, steady film flow but time-dependent, irregular film flow. Then we present the experimental study of continuous film flow using frames with trapezoidal apertures (asymmetric frames). Finally, a numerical study of these film flows is presented, which is based upon the induced-charge mechanism in ohmic liquids.

*Corresponding author: mnasiri@znu.ac.ir

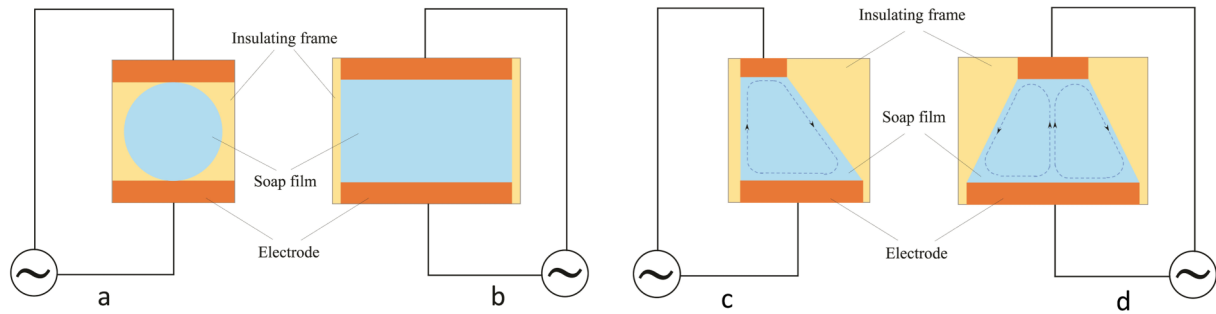


FIG. 1. Schematic of experiments for symmetric [circular (a) and rectangular (b)] and asymmetric [right-angled trapezoidal (c) and isosceles trapezoidal (d)] apertures.

II. MATERIAL AND METHODS

A. Material

In this work, soap films are made of water, glycerin, and ammonium lauryl sulfate (ALS) solution. ALS is an anionic surfactant that we purchased from Fluka as an ALS solution, 30% in water. We dissolved 0.2 ml of the ALS solution and 10 ml of glycerol in 100 ml of DI water. The critical micellar concentration (cmc) for the surfactant is 0.00075 M, and the surfactant concentration in the solution we used in experiments is above the cmc. The viscosity and electrical conductivity of the final solution are 1.24 mPa · s and 0.018 S/m, respectively.

B. Particle image velocimetry

Fluid flow velocity in the soap film is measured by a process similar to particle image velocimetry (PIV). The recorded images show a color pattern due to small spatial variations of film thickness. This color pattern follows the liquid film motion. The thickness of soap films depends on position and decreases with time. This thickness can be measured by interferometry or estimated from the interference colors observed on the film. The film thickness can range from ~ 0.1 to $\sim 10 \mu\text{m}$. The film thinning is spontaneous due to evaporation or draining. The flow of soap films was recorded by a high-speed camera (Casio Exilim EX-ZR200) at the rate of 120 frames per second. For each measurement, we have taken 10 consecutive images with a time separation of 0.008 s.

III. EXPERIMENTAL DETAILS

A. Apertures for producing soap films

To apply an electric voltage difference on soap films, we use an insulating frame which is coated with copper. An aperture of deliberate shape is made by laser cutting where the soap film will be suspended. The frame thickness is 1 mm. By removing the conducting coating from some parts of the insulating frame, the aperture is limited by electrodes separated by insulators (see Fig. 1). A soap film is formed by drawing a rod wetted by the soapy solution over the produced aperture. The soap film is held horizontally, and it is in contact with the surrounding air from above and below. Due to the absence of constraints on the film, it can be readily set into motion by application of very small force.

In this work, we have used four different apertures: two symmetric and two asymmetric. The symmetric apertures have either circular or rectangular shapes. The asymmetric apertures have either right-angled trapezoidal or isosceles trapezoidal

shapes. The electrodes are placed at two opposite sides of the rectangular frame. We have investigated the flow generated on freely suspended soap film by applying either ac or dc electric voltage difference between the electrodes, which are in contact with the soap film.

B. Applied electric voltages

In order to apply an ac electric voltage difference between the electrodes, we use a power supply capable of producing a square wave shape of amplitude up to 250 V (root mean square) and signal frequency between 7 and 103 Hz. In order to apply a dc electric voltage, we use a dc power supply with variable voltage from 0 to 2 kV. The voltage is applied between the coated copper electrodes schematically shown in Fig. 1.

IV. EXPERIMENTAL RESULTS

Our experiments show that by applying a sufficiently large ac or dc electric voltage difference between the electrodes, which are in contact with the soap film, some flows on the film can be observed. Our observations show that the flow pattern depends on the shape of electrodes and aperture. In order to reduce possible electrochemical effects, we perform the measurements at the early stages of the experiments.

A. Symmetric apertures

By applying an ac or dc voltage difference to the electrodes of frames with symmetric apertures (circular or rectangular as shown in Fig. 1), some complicated time-dependent patterns of motion are observed in the film (see Figs. 2 and 3). Flow velocity increases as we increase the electric voltage difference. The measured PIV at two different times reveals that the soap film flow is time dependent for these symmetric apertures (see Figs. 2 and 3). This behavior is the same for both ac and dc electric voltage. These irregular flows could be originated by electrohydrodynamic instabilities, although they can also be due to inhomogeneities along the film (of thickness, surface tension, etc).

B. Asymmetric apertures

In this work, we use two asymmetric apertures where the soap films are suspended. One is right-angled trapezoidal (height = 6 mm and parallel sides = 3 and 9 mm), and the other is isosceles trapezoidal (height = 6 mm and parallel sides = 3 and 10 mm) as shown in Fig. 1. Our experiments show that by applying ac or dc electric voltage difference to the asymmetric apertures, steady vortices are generated in the film, in contrast to the symmetric cases. For the right-angled

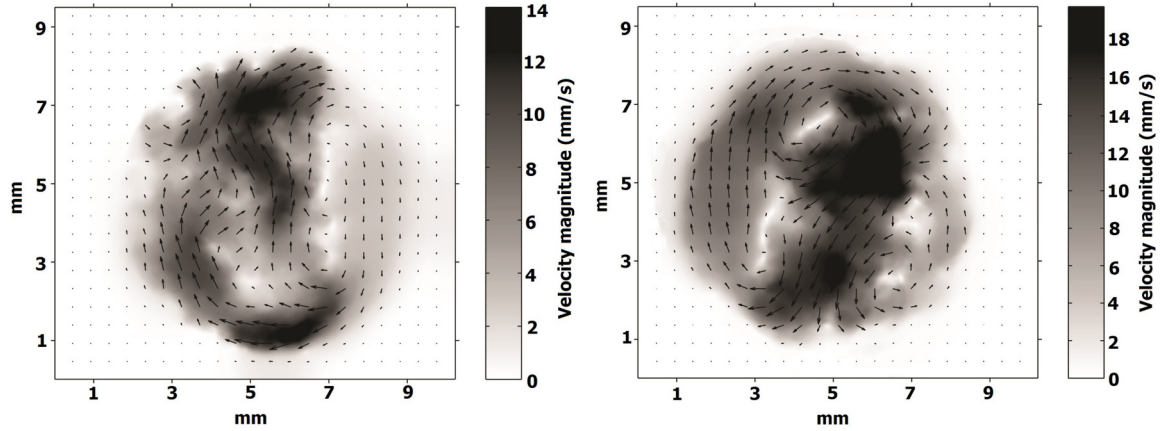


FIG. 2. PIV of soap film flow in a circular aperture in two instants of time, with an interval of 1.5 s. The frequency and root mean square of voltage are 6.5 Hz and 250 V, respectively.

trapezoidal aperture there is a dominant vortex [see Fig. 4(a)], and for the isosceles trapezoidal aperture there are two dominant rotating opposite vortices [see Fig. 4(b)]. Our observations show that by changing the applied dc electric voltage polarity, the direction of rotating flow does not change. In addition, by switching between ac or dc applied electric voltage to the asymmetric aperture, no noticeable difference was observed in the soap film flow; i.e., the time-independent flow pattern was very similar in ac or dc modes. This suggests that the flow is due to the induced charge mechanism, where the electric field actuates on the charge that is induced by itself. The charge induction mechanism is very well established and appears in many different electrohydrodynamic experiments. The classical Taylor pump is a very clear example of it [24,25]. The flow velocity magnitude increases with the applied ac or dc voltage difference, and the flow direction depends only on the aperture geometry. The velocity field of the soap film flow induced by an applied ac voltage is shown in Fig. 5 for right-angled and isosceles trapezoidal apertures. The soap film rolls in both apertures show very similar behavior with respect to the applied signal. Therefore, we concentrated on the right-angled trapezoidal aperture for the quantitative measurements of soap film flow.

C. Frequency and voltage dependence of the motion

Our experiments for soap film show that the flow in the right-angled trapezoidal aperture is only slightly dependent on

the frequency of applied ac voltage. Figure 6 shows the average angular velocity, Ω , versus the applied signal frequency for a constant voltage amplitude of 250 V (rms). As can be seen, the velocity of rotation is almost independent of the applied signal frequency. In addition, it was observed that the flow velocity is almost the same for ac or dc applied voltage. Figure 6 shows that the flow velocity is proportional to the square of voltage amplitude (either dc or ac) for the right-angled trapezoidal aperture. The figure shows in a log-log plot the average angular velocity versus applied voltage amplitude (rms) for a constant frequency of 6.5 Hz. The fact that velocity amplitude is proportional to the square of applied voltage is also an indication of induced charge mechanism, where the electric field actuates on its own induced charge.

V. THEORY AND NUMERICAL SIMULATION

In this section, we employ the leaky dielectric model to describe the electrohydrodynamics of the fluid film [26]. In this model, the fluid film is characterized by its electrical conductivity and dielectric permittivity. The applied electric field induces charges at upper and lower interfaces of the film. This induced charge is considered to be superficial, although, in reality, it extends to some distance inside the film on the order of the Debye length λ_D . Important for the derivation of the leaky dielectric model is that the Debye length is much smaller

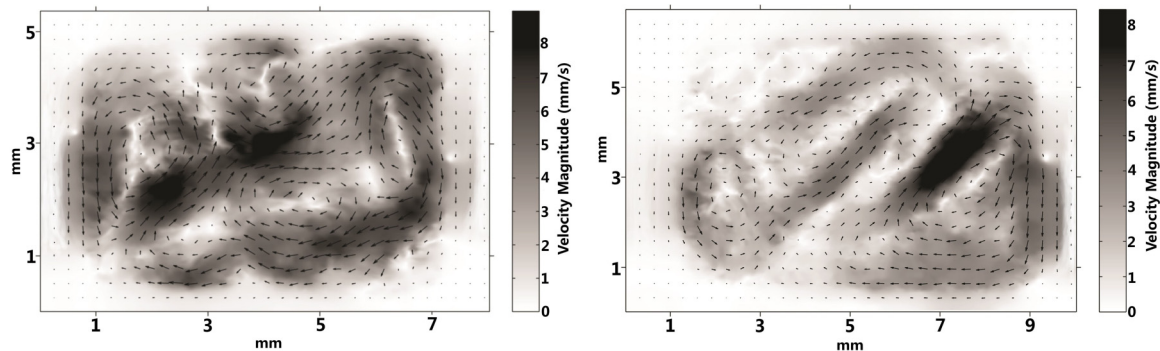


FIG. 3. PIV of soap film flow in a rectangular aperture in two instants of time, with an interval of 2 s. The frequency and root mean square of voltage are 6.5 Hz and 250 V, respectively.

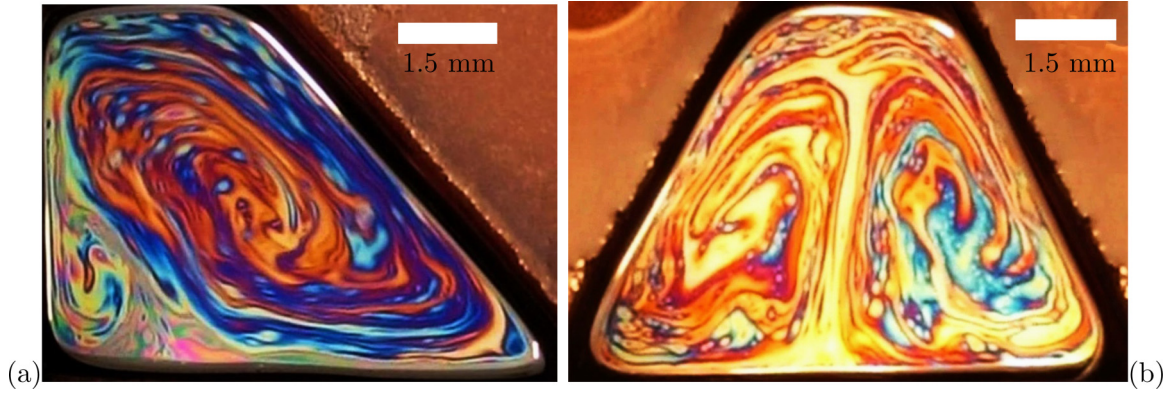


FIG. 4. Applied voltage in a right-angled-trapezoid aperture is dc and the voltage is 500 V. For an isosceles trapezoid, the frequency and root mean square of applied voltage are 6.5 Hz and 100 V, respectively.

than the characteristic length of the system. In the experiments, the electrical conductivity is such that we estimate the Debye length to be on the order of 10 nm. This is much smaller than the film thickness, $d \sim 0.1\text{--}1\ \mu\text{m}$. In this work, we suppose that surface tension provides the normal stability of the film, and we neglect the effect of surface tension on the fluid motion. Other simplifications in the numerical study are considering constant thickness of the fluid film and neglecting nonuniform distribution of surfactant.

In the proposed two-dimensional (2D) simulation of the fluid film we neglect the effect of menisci of the film, which can be important, especially on the frame boundaries. Although we have worked with frames with different thicknesses, the experimental results were similar. For the experiments in Sec. V the frame thickness is 1 mm. Taking into account the effect of film thickness profile requires a three-dimensional (3D) finite element simulation, which is more challenging and time consuming for thin films. Our expectation is that the effect extends a distance about 1 mm from the frame boundaries. However, we observe that the flow velocity is zero near the frame in the experiments. This is in accordance with the boundary condition ($\mathbf{u} = 0$) that we impose on the frame boundaries.

The governing electric and hydrodynamic equations will be solved using the commercial finite element solver COMSOL. The simulation domain consists of a 2D fluid film (right-angled or isosceles trapezoid) surrounded by $16 \times 16 \times 8$ mm

air box. The electrodes are placed at two opposite sides of the rectangular frame as in Fig. 1 and connected to ac voltage $\pm V_0 \sin(\omega t)/2$, respectively, where V_0 and $\omega = 2\pi f$ are the amplitude and angular frequency of the applied signal, respectively.

Inside the air box the governing equation is the continuity of the total (ohmic plus displacement) electrical current that in phasor notation reads

$$\nabla \cdot (\sigma \mathbf{E} + i\omega \epsilon_0 \mathbf{E}) = 0, \quad (1)$$

where \mathbf{E} is the phasor of the electrical field, and $\epsilon_0 = 8.85 \times 10^{-12}$ F/m is the permittivity of air. The electrical conductivity of air is negligible so that $\sigma = 0$ in previous equation. In our problem, magnetic fields can be ignored completely and the electric field is irrotational, $\mathbf{E} = -\nabla\phi$, where ϕ is the electric potential phasor.

The fluid film is an ohmic medium with permittivity $\epsilon_{\text{film}} = 80\epsilon_0$ and electrical conductivity $\sigma_{\text{film}} = 0.018$ S/m. The film is a thin layer of water and glycerol mixture with thickness $d = 1\ \mu\text{m}$, which is very small in comparison with the size of the surrounding air box. This great difference in lengths allows us to consider the film as bidimensional and to take it into account in the electrical problem as a boundary condition [21]:

$$\mathbf{n} \cdot (\mathbf{J}_2 - \mathbf{J}_1) = -\nabla_s \cdot [d(\sigma_{\text{film}} + i\omega \epsilon_{\text{film}})\nabla_s \phi]. \quad (2)$$

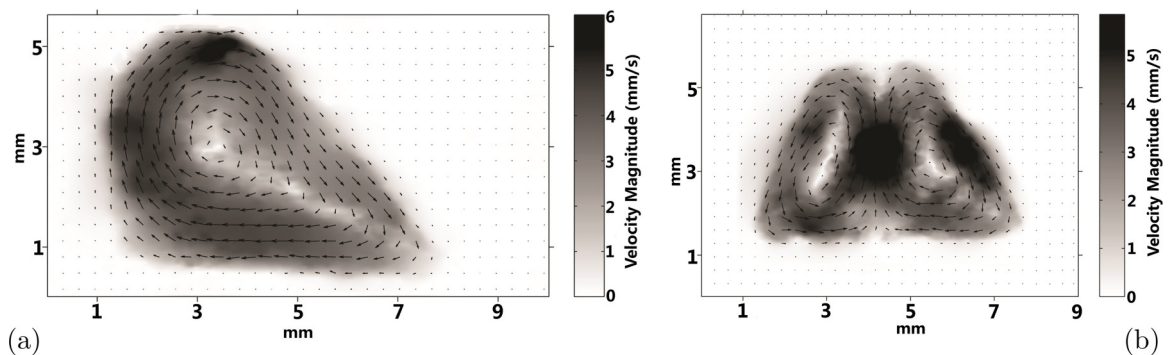


FIG. 5. PIV of a soap film flow in right-angled-trapezoidal (left) and isosceles-trapezoidal (right) apertures. In a right-angled-trapezoid aperture, the frequency and root mean square of applied voltage are 100 Hz and 250 V, respectively, and in an isosceles-trapezoid aperture, the frequency and root mean square of applied voltage are 6.5 Hz and 100 V, respectively.

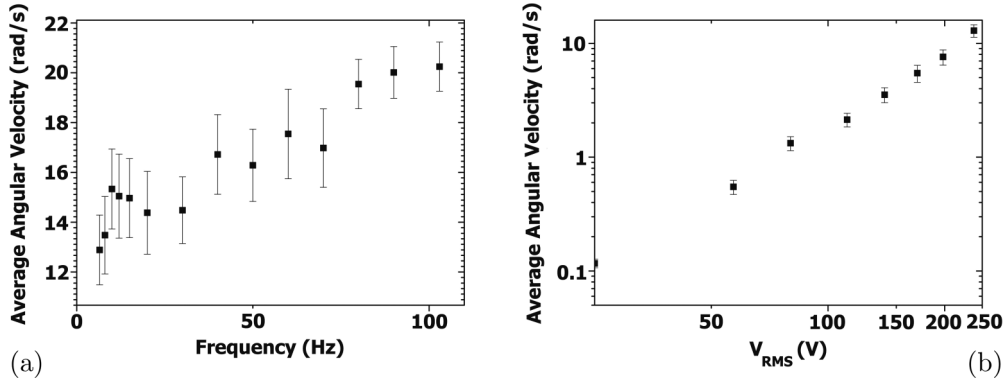


FIG. 6. (a) Average angular velocity vs the applied voltage frequency. The root mean square of applied voltage is 250 V. (b) Average angular velocity vs root mean square of applied voltage. The frequency of applied voltage is 6.5 Hz.

Here \mathbf{n} is the normal vector pointing from the lower to the upper region of the surface, \mathbf{J}_2 and \mathbf{J}_1 are the total current densities in the upper and lower regions, respectively, and ∇_s denotes the tangential nabla operator acting on the fluid film. The remaining boundary conditions are those of fixed potential $\pm V_0/2$ at the electrodes and normal total current equal to zero at outer surfaces. Once the electric field is obtained, the induced surface charge on the film at low frequencies ($\epsilon_{\text{film}}\omega \ll \sigma_{\text{film}}$) can be obtained from the discontinuity of the electric displacement field normal component:

$$q_s = \epsilon_0(\mathbf{E}_2 - \mathbf{E}_1) \cdot \mathbf{n}. \quad (3)$$

Here \mathbf{E}_2 and \mathbf{E}_1 are the electric fields on both sides of the film. The motion of the fluid film can be obtained by solving a 2D fluid problem that includes a Coulomb force actuating on the surface charge. The 2D fluid is characterized by $\bar{\rho} = \rho d$ and $\bar{\eta} = \eta d$, the 2D mass density and viscosity, respectively. In steady state the 2D fluid flow $\mathbf{u} = (u, v)$ is governed by the Navier-Stokes and continuity equations as follows:

$$\bar{\rho}(\mathbf{u} \cdot \nabla_s)\mathbf{u} = -\nabla_s \bar{p} + \bar{\eta} \nabla_s^2 \mathbf{u} + \mathbf{F}_e, \quad (4)$$

$$\nabla_s \cdot \mathbf{u} = 0, \quad (5)$$

where $\bar{p} = pd$ is the 2D pressure field and $\mathbf{F}_e = \langle q_s \mathbf{E}_s \rangle$ is the time-averaged tangential electrical stress acting on the 2D fluid. We assume no slip, $\mathbf{u} = 0$, boundary conditions on all

sides of fluid film and low Reynolds regime, $\text{Re} \ll 1$, which allows us to neglect the nonlinear term in Eq. (4). We have used the time-averaged electrical force because signal periods are much shorter than typical mechanical times. Using phasors, the time-averaged Coulomb force is given by

$$\mathbf{F}_e = \frac{1}{2} \text{Re}(q_s \mathbf{E}_s^*), \quad (6)$$

where $\text{Re}(\dots)$ denotes the real part and \mathbf{E}_s^* is the complex conjugate of tangential electric field on fluid film.

VI. RESULTS

Distribution of surface charge induced by an electric field for asymmetric frames is calculated and shown in Fig. 7. The values of the physical parameters used for the numerical simulation are provided in Table I. Figures 8(a) and 8(b) show the velocity vector field for frames with right-angled and isosceles trapezoidal apertures, respectively. The flow patterns are in accordance with those shown in Fig. 5, especially with respect to the direction of the fluid motion. In the case of a right-angled trapezoid there is a dominant vortex rotating clockwise, and for the isosceles trapezoid there are two dominant vortices.

We use vorticity of the flow field to compare the simulation and experimental results. In fluid mechanics the vorticity at a point is twice the velocity of the fluid particle around that point $\nabla \times \mathbf{u} = 2\Omega$, where $\nabla \times \mathbf{u}$ and Ω are local vorticity and angular velocity, respectively. Figure 9 depicts the average

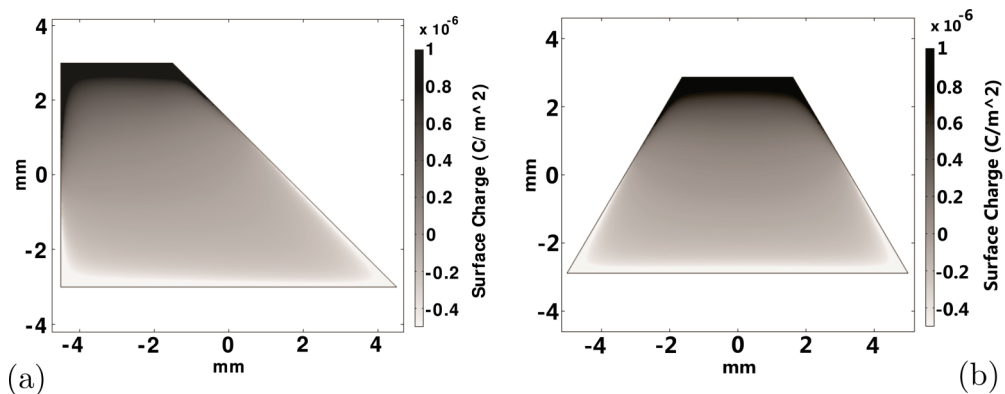


FIG. 7. (a) and (b) Surface charge distribution in C/m^2 of right-angled and isosceles trapezoidal frames. $V_0 = 100$ V and $f = 6.5$ Hz, and physical parameters of the film can be seen in Table I.

TABLE I. Values of physical parameters in numerical simulation.

Film bulk viscosity η (mPa · s)	1.24
Film thickness d (μm)	1
Film conductivity σ (S/m)	0.018
Dielectric constant of film (ϵ_r)	80

vorticity of flow versus voltage amplitude V_0 in a log-log plot for $f = 6.5$ Hz measured along a small line from $(-1,0)$ to $(0,0)$ for the right-angled trapezoidal aperture. The figure also shows the experimental angular velocity. The figure shows that the vorticity scales as V_0^2 , which is almost in accordance with Fig. 6. The power law scaling of the vorticity with voltage clarifies that, in a first approximation, the role of electroosmosis should be negligible in front of the induced charge mechanism in order to describe the fluid flow.

Although the simulated and experimental average vorticity versus voltage are in accordance qualitatively, computed velocities are about 10 times higher than in experiments. The 2D viscosity obtained from the bulk viscosity of the ALS solution and the film thickness is $\bar{\eta} = 1.24 \times 10^{-9}$ Pa · s · m, and the effective 2D viscosity that fits experiments and computations is $\bar{\eta} = 1.4 \times 10^{-8}$ Pa · s · m. The main factor that could account for the discrepancy [19] is contribution of surfactants to the effective surface viscosity of the fluid film [27]. The effective surface viscosity of a film is given by $\bar{\eta}_{eff} = d\eta_{3D} + 2\bar{\eta}_{in}$, where $\bar{\eta}_{in}$ is the 2D surface viscosity of the two surfactant-laden interfaces and η_{3D} is the bulk viscosity. Regarding some experimentally accessible values for $\bar{\eta}_{in}$ and η_{3D} , one can conclude that the surface viscosity could be sufficient to conform theory and experiments [19,28].

With respect to the symmetric frames, we have computed the induced charge distribution on the film for the rectangular frame. The isolines of this induced charge are almost parallel to the electrodes. The electric field that actuates on this charge is almost perpendicular to these isolines, since it follows the ohmic current density inside the film that goes straight from one to the other electrode. This creates an electrical force that is very homogeneous and that can almost be equilibrated by a static pressure distribution alone, without giving rise to a fluid motion. The amplitude of fluid flow computed from this force is much smaller than the one in the case of asymmetric electrodes

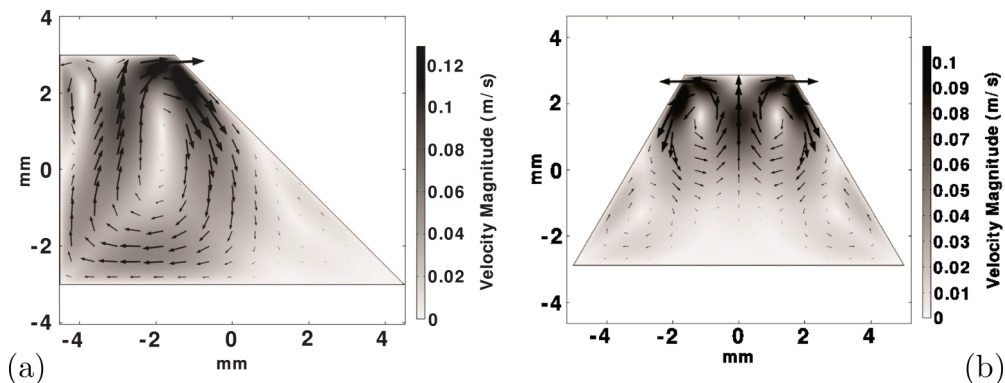


FIG. 8. Velocity magnitude in m/s and vector field. (a) Case of a right-angled trapezoid, $V_0 = 100$ V and $f = 6.5$ Hz. (b) Case of an isosceles trapezoid, $V_0 = 200$ V and $f = 6.5$ Hz. Physical parameters of the film can be seen in Table I.

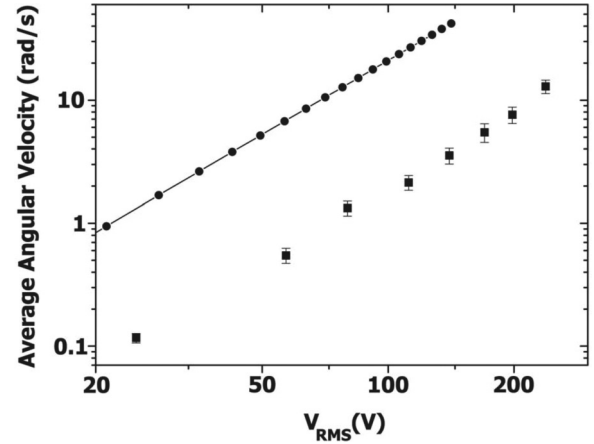


FIG. 9. Simulated average angular velocity (solid line) and experimental angular velocity as a function of voltage (points) for the right-angled trapezoid and for an applied signal of $f = 6.5$ Hz. Physical parameters of the film are shown in Table I.

and consists of four rolls. We think that this flow pattern is masked by the time-dependent flow observed in experiments.

VII. CONCLUSIONS

Controllable net fluid flow of soap films induced by (ac or dc) electric fields in asymmetric frames has been presented. Previous experiments with soap films employed either the simultaneous use of an electrical current passing through the film and an external electric field or nonuniform ac electric fields in order to obtain controllable fluid film flow. Here a single voltage difference has been used to generate both the electrical current going through the film and the electric field that actuates on the charge induced on the film. The film is set into global net motion due to the broken symmetry of asymmetric frames. When symmetric frames are used instead, the film flow was not steady but time dependent and irregular. Finally, we have studied numerically these film flows by employing the model of charge induction in ohmic liquids, and we have found qualitative agreement with the experimental observations.

ACKNOWLEDGMENTS

We would like to acknowledge A. Nejati for helpful discussions. A.R. acknowledges financial support by the Spanish

Government Ministry MEC under Contract No. FIS2014-54539-P.

-
- [1] H. A. Stone, A. D. Stroock, and A. Ajdari, *Annu. Rev. Fluid Mech.* **36**, 381 (2004).
- [2] T. M. Squires and S. R. Quake, *Rev. Mod. Phys.* **77**, 977 (2005).
- [3] D. R. Arifin, L. Y. Yeo, and J. R. Friend, *Biomicrofluidics* **1**, 014103 (2007).
- [4] A. Manz, N. Graber, and H. Widmer, *Sensors Actuators B* **1**, 244 (1990).
- [5] M. P. Hughes, *Nanotechnology* **11**, 124 (2000).
- [6] O. Bonhomme, O. Liot, A.-L. Biance, and L. Bocquet, *Phys. Rev. Lett.* **110**, 054502 (2013).
- [7] O. Bonhomme, B. Blanc, L. Joly, C. Ybert, and A.-L. Biance, *Adv. Colloid Interf. Sci.* **247**, 477 (2017).
- [8] M. Gharib and P. Derango, *Physica D* **37**, 406 (1989).
- [9] J. M. Chomaz and B. Cathalau, *Phys. Rev. A* **41**, 2243(R) (1990).
- [10] M. Rutgers, R. Bhagavatula, A. Petersen *et al.*, *Phys. Fluids* **8**, 2847 (1996).
- [11] S. Faetti, L. Fronzoni, and P. Rolla, *J. Chem. Phys.* **79**, 5054 (1983).
- [12] S. Faetti, L. Fronzoni, and P. Rolla, *J. Chem. Phys.* **79**, 1427 (1983).
- [13] S. W. Morris, J. R. de Bruyn, and A. D. May, *Phys. Rev. Lett.* **65**, 2378 (1990).
- [14] Z. A. Daya, S. W. Morris, and J. R. de Bruyn, *Phys. Rev. E* **55**, 2682 (1997).
- [15] A. Amjadi, R. Shirsavar, N. H. Radja, and M. R. Ejtehad, *Microfluidics Nanofluidics* **6**, 711 (2009).
- [16] R. Shirsavar, A. Amjadi, A. Tonddast-Navaei, and M. R. Ejtehad, *Exp. Fluids* **50**, 419 (2010).
- [17] R. Shirsavar, A. Amjadi, M. R. Ejtehad, M. R. Mozaffari, and M. S. Feiz, *Microfluidics Nanofluidics* **13**, 83 (2012).
- [18] T. Saghaei, A.-R. Moradi, R. Shirsavar, and M. Habibi, *Appl. Phys. Lett.* **106**, 053506 (2015).
- [19] M. Nasiri, R. Shirsavar, T. Saghaei, and A. Ramos, *Microfluidics Nanofluidics* **19**, 133 (2015).
- [20] R. Shirsavar, A. Ramos, A. Amjadi, J. Taherinia, M. Mashhadi, and A. Nejati, *J. Electrostat.* **73**, 112 (2015).
- [21] M. Nasiri, R. Shirsavar, S. Mollaei, and A. Ramos, *Phys. Rev. E* **95**, 022806 (2017).
- [22] A. Ajdari, *Phys. Rev. E* **61**, R45 (2000).
- [23] T. M. Squires and M. Z. Bazant, *J. Fluid Mech.* **560**, 65 (2006).
- [24] J. Melcher and G. Taylor, *Annu. Rev. Fluid Mech.* **1**, 111 (1969).
- [25] O. A. Basaran and L. E. Scriven, *Chem. Eng. Commun.* **67**, 259 (2007).
- [26] D. Saville, *Annu. Rev. Fluid Mech.* **29**, 27 (1997).
- [27] V. Prasad and E. R. Weeks, *Phys. Rev. E* **80**, 026309 (2009).
- [28] P. Stevenson, *J. Colloid Interf. Sci.* **290**, 603 (2005).